J Mater Sci: Mater Electron (2017) 28:9763–9769
DOI 10.1007/s10854-017-6728-6

Medium temperature sintered $BaTiO_3$-based X8R ceramics with Bi_2O_3–TiO_2–ZnO–H_2BO_3 additive

Lingxia Li[1] · Jiangteng Li[1] · Ning Zhang[1] · Zhaoyang Cai[1] · Bowen Zhang[1] · Weijia Luo[1]

Received: 4 January 2017 / Accepted: 10 March 2017 / Published online: 22 March 2017

Abstract Lead-free medium temperature sintering $BaTiO_3$-based X8R ceramic materials were obtained by sintering with addition of nano-size Bi_2O_3–TiO_2–ZnO–H_2BO_3(BTZB), which was synthesised successfully via a sol–gel method. and showed high activity and great dispersion properties. Moreover, the dielectric property and bulk densities was also influenced by the BTZB nanopowder content. The results indicate that BTZB nanopowders can be used as a sintering aid to reduce the sintering temperature of $BaTiO_3$ from 1300 to 1150 °C without secondary phase formation. The 4 wt% BTZB-doped sample which sintered at 1150 °C showed super dielectric properties that the dielectric constant $\varepsilon_r = 3186$ at 25 °C and dielectric loss was lower than 1.5%. the temperature stability was also improved, temperature coefficient of capacitance less than ±15% from −55 to 150 °C, meeting X8R standard.

1 Introduction

With the rapid development of the electronics industry, techniques for producing multilayer ceramic capacitor (MLCC) with large capacitance and small size have been further improved. The material systems with higher Curie temperatures are desirable for MLCC applications at harsh working condition such like military industry, instrument and aerospace, oil exploration. In such condition, X8R ceramics (55–150 °C, $\Delta C/C_{20℃} \leq 15\%$) are of increasing importance in the rapidly developing electronics industry .

The development tendency of multi-layer ceramic capacitors (MLCCs) is high-capacitance with small size, which requires the dielectric materials achieving higher permittivity with a uniform grain size. Consequently, X8R MLCC have been widely used for miniaturization of electronic components due to their high dielectric constant and temperature-stable dielectric characteristics [1].

It's very suitable to make MLCC with $BaTiO_3$ due to its' high dielectric constant at room temperature [2].However, according to the Curie–Weiss law, pure $BaTiO_3$ dielectric constant curve have a sharp drop when temperature higher than 125 °C, which cannot meet the requirement of X8R. Thus,It's very important to find out the variation trend of the Curie point of $BaTiO_3$-based ceramics to improve the temperature stability.

High-performance X8R ceramics usually result from the formation of a ''core–shell'' structure, with the core being a pure $BaTiO_3$ ferroelectric phase and the shell of paraelectric phase. It's difficult to obtain mature matrix at low temperature, so that high temperature is required. However, the ''core–shell'' structure of ceramics might be destroyed and form a single solid solution when sintered at excess temperature, which might make it not satisfy X8R characteristics. Besides, noble metals, such like Pd, Pt and Au, are used in the process at high temperature as traditional internal electrodes, which are extremely expensive, will increase the cost of MLCCs, consequently, noble metal is not a good option for the commercial production of MLCCs. Accordingly, it's important to obtain a compact ceramic with intact ''core–shell'' structure at lower temperature. Nowadays, the effective approach to enhance densification sintering and improving dielectric property is using sintering aids with a low melting point during the sintering process. Two

✉ Lingxia Li
llx666_tju@126.com

[1] Key Laboratory for Advanced Ceramics and Machining Technology, Ministry of Education and School of Electronic and Information Engineering, Tianjin University, Tianjin 300072, China

types of sintering aids are commonly used. One of them is single oxide, such like ZnO [3] or Bi_2O_3 [4].Another type of sintering aids is composite oxide, such like B_2O_3–SiO_2 [5], ZnO–B_2O_3–SiO_2 [6] or BaO–CaO–B_2O_3–SiO_2 [7]. As we know, composite oxides are more efficiency to lower the sintering temperature compared with single oxides. Furthermore the addition of composite oxides plays an important role in improving dielectric properties of ceramics and modification of the microstructure, and for this reason, composite oxides using as sintering aids has been widely studied.

The melt-quench technique, a solid-state method, is the most economical and mostly used method to prepare sintering aids, which will form large and irregular particles [8]. In general, larger amount of micron or submicron size oxides doping to ceramics compared with nanoscale oxides, will caused reduction of ceramic density and dilution of ferroelectric phase, which could lead to a significant reduction of dielectric property [9].As a result, a suitable sintering aid with nanoscale particles size is quite important to reduce the sintering temperature and enhance densification without reduction of dielectric properties of the ceramic material.

Single oxide sintering aids with low melting temperature, such as ZnO [3], Bi_2O_3 [4] were used to enhance the densification, and TiO_2, a component of $BaTiO_3$, was used to improve solid solubility. Besides, Bi_2O_3–ZnO–H_2BO_3, with a low melting temperature, has a great modified ability to improve the dielectric property and microstructure of $BaTiO_3$-based ceramics as sintering aids. Therefore, Bi_2O_3–TiO_2–ZnO–H_2BO_3 (BTZB) nanopowders were synthesized via sol–gel technique, which was then used as a sintering aid to produce $BaTiO_3$-based ceramics at a low temperature with good dielectric property.

2 Experimental

2.1 Sample preparation

The BTZB nanopowders were synthesized by the sol–gel process. Analytically pure (AR) bismuth nitrate [$Bi(NO_3)_3{\cdot}5H_2O$, ≥99.0%],tetrabutyl titanate ($C_{16}H_{36}O_4Ti$, ≥99.0%),zinc nitrate hexahydrate [$Zn(NO_3)_2{\cdot}6H_2O$, ≥99.0%] and boric acid (H_3BO_3,≥99.0%) were used as the raw materials. Citric acid and ethylene glycol were used as a chelating agent and reaction medium. Nitric acid is chosen to adjust the pH of sol because it is a strong acid and decomposes easily without harmful ions. The synthesizing route for preparing the BTZB nanopowders was shown in Fig. 1.The base material was $BaTiO_3$ powder (Guoci Co. Ltd., China).The additives included 0.2 wt % Niobium and manganese compounds (synthesized from $MnCO_3$ and Nb_2O_5 with the mole ratio of 2:1), 0.9 wt % Niobium and nickel compounds (synthesized from NiO and Nb_2O_5 with the mole ratio of 3:4), and various amounts of BTZB nanopowders (0.0, 1.5, 3.0, 4.0 and 5.0 wt %). $BaTiO_3$ and all the additives were weighed and mixed with deionized water

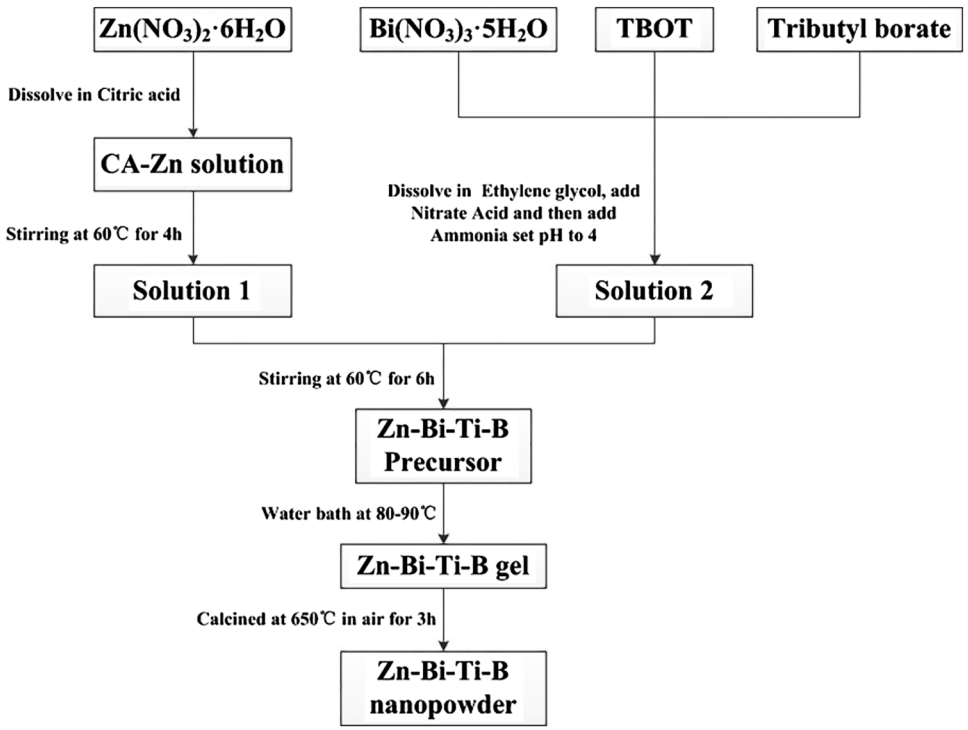

Fig. 1 Flow chart for preparing the BTZB nanopowders by the sol–gel process

by ball milling (using ZrO_2 millball) for 4 h and then dried. After drying, mixed powders were added in 7.0 wt% binder wax, and then pressed into disks with 15 mm in diameter and 1 mm in thickness. The sample with 1.5–5.0 wt% BTZB nanopowders were named A15–A50 sintered at 1150 °C for 3 h in air, sample A00 with no BTZB sintered at 1300 °C for 3 h in air, using a heating rate of 5 °C/min. Silver was applied on both sides of the as-fired samples to obtain the electrodes of capacitors.

2.2 Characterization

Dielectric loss and the capacitance were measured by the use of capacitance meter (HP4278A; Hewlett Packard, Santa Clara, CA) at 1 kHz from −55 to 150 °C. The TCC value is calculated by using the equation $\Delta C/C_{20\,^{\circ}C} = (C - C_{20\,^{\circ}C})/C_{20\,^{\circ}C} \times 100\%$, where $C_{20\,^{\circ}C}$ is the capacitance at 20 °C, and C is the capacitance of either temperature in the range of −55–150 °C The temperature was controlled by GZ-ESPEC oven. Insulation resistivity was measured using a high resistance meter (Agilent4339B, Santa Clara, CA) at room temperature. The frequency characteristics were measured between 50 Hz and 100 kHz, using a TH2828S automatic component analyzer. Phase identification and lattice parameters were characterized by X-ray diffraction (XRD) patterns, which were obtained from an D/MAX-B Model X-ray diffractometer (D8-Focus; Bruker AXSGmbH, Karlsruhe, German) with CuKa radiation at 40 kV and 40 mA. Microstructural properties such as grain size distribution and morphology were examined using a field-emission scanning electron microscopy (FE-SEM, S-4800; Hitachi, Ltd., Tokyo,Japan). The bulk density of the samples was measured by an Archimedes method.

3 Results and discussion

3.1 Solubility analysis

We verified the crystal structure of these mixtures by means of XRD (Fig. 2). The XRD results demonstrate that all the samples display a desired perovskite structure, which indicates that the BTZB have diffused into the $BaTiO_3$ lattice to form a stable solid solution. And there was obvious splitting for peaks at $2\theta = 45.5°$ in sample A15 A30 and A00. indicating that the ceramics mainly consisted of a tetragonal phase while sample A40 and sample A50 both showed a pseudo-cubic structure with a single peak of (200).With the increasing BTZB content the (200) and (002) peaks emerge into one peak as shown in Fig. 2. As we know, the tetragonal structure is characterized by (200) and (002) peak splitting around 45°, and the pseudo-cubic structure is characterized by (200) peak around 45° [10, 11]. As a result, according to these characteristic peaks, it shows that the crystal structure changes gradually from tetragonal to pseudo-cubic with increasing BTZB content.

The secondary phase ($Ba_6Ti_{17}O_{40}$ (JCPDF 77-1566)) was detected in sample A00 with no BTZB sintered at 1300 °C, Because $(Ni_{1/3}{}^{2+}Nb_{2/3}{}^{5+})^{4+}$ composite cation would easily diffuse into the crystal lattice and replace the Ti^{4+} cation, and the excess Ti^{4+} cation reacts with the $BaTiO_3$ and forms a $Ba_6Ti_{17}O_{40}$ (JCPDF77-1566) second phase [12]:

$$6BaTiO_4 + 11Ti^{4+} + 16O^{2-} \rightarrow Ba_6Ti_{17}O_{40}$$

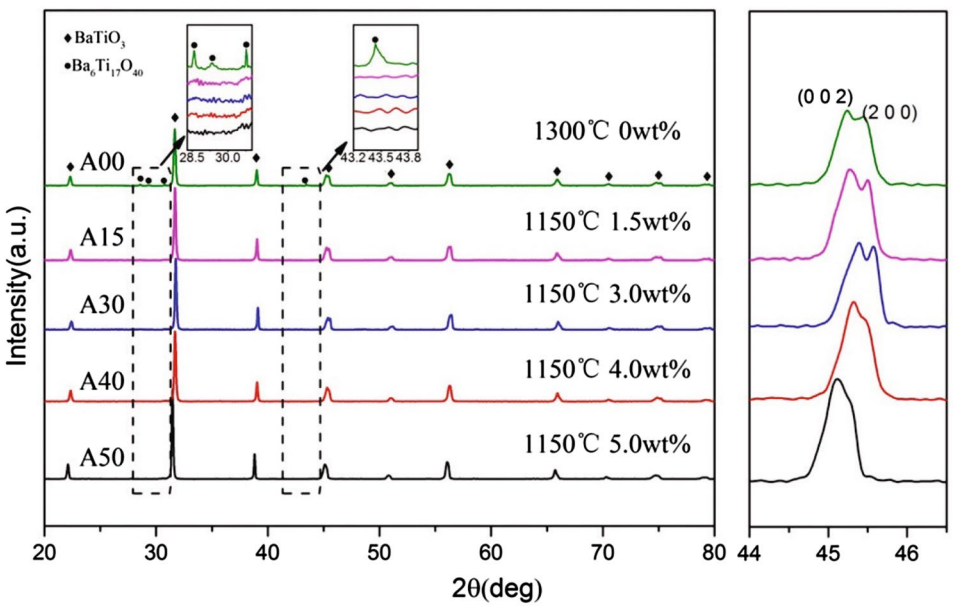

Fig. 2 XRD patterns of $BaTiO_3$ samples doped with various amounts of BTZB sintered at 1150 °C and $BaTiO_3$ sample with no BTZB sintered at 1300 °C

There is no new phase appeared in other samples, which indicating that the addition of BTZB nanopowders inhibits the form of the $Ba_6Ti_{17}O_{40}$ second phase, during sintering process, BTZB diffused into the $BaTiO_3$ ceramics system, and the BTZB formed a liquid phase due to their melting temperature and the high reactivity of its nano-particles, which was lower than that of the surrounding matrix; this promotes a solid state reaction during the prophase of sintering which will promote Ba^{2+} cations' migration rate and reacts with the $Ba_6Ti_{17}O_{40}$:

$$Ba_6Ti_{17}O_{40} + 11Ba^{2+} + 11O^{2-} \rightarrow 17BaTiO_4$$

Therefore BTZB can inhibit the formation of the $Ba_6Ti_{17}O_{40}$ second phase, Moreover, BTZB particles are likely to interact with $BaTiO_3$ at the grain boundaries during the late-stage of sintering phase. Which will promote the sintering process and reduce the sintering temperature of $BaTiO_3$ [13].

The effect of the BTZB content on the unit cell of $BaTiO_3$ estimated from XRD pattern is shown in Fig. 3,as we can see, with an increase of BTZB content, the volume of a unit cell decreases nearly linearly from 64.4219 to 62.9789 $Å^3$. The decrease of the unit cell volume can be explained that BTZB doping result in the substitution of smaller Bi^{3+} ions (1.02 Å) with the Ba^{2+} (1.61 Å) sites of $BaTiO_3$. This linear relationship also indicates that up to 5 wt% of BTZB has completely incorporated into the $BaTiO_3$ lattice. Consequently, no second phase formation in sample A15–A50, which was consistent with the change in XRD patterns and SEM micrographs.

The degree of tetragonality can be quantified by the c/a ratio, c and a are the lattice parameters of tetragonal perovskite). The results in Fig. 3 show that the c/a ratio decrease from 1.00421 to 1.00226 when the BTZB content increases from 1.5 to 4.0 wt%, which indicate that the crystal structure changes gradually from tetragonal to pseudo-cubic with increasing BTZB content from 1.5 to 4.0 wt%.

Then, the c/a ratio increases from 1.00226 to 1.00407 when the BTZB content increases from 4.0 to 5.0 wt%. Correspondingly, it's possible that the change of crystal structure in this system is caused by the lattice mismatch between a pure $BaTiO_3$ crystal region (core) and a Bi^{3+} ion incorporated region (shell),which was causing an internal stress and inhibits the phase transition from tetragonality to cubic and increase tetragonality (c/a ratio) [14].

3.2 Microstructure analysis

The particle sizes and morphology of the BTZB nanocomposite synthesized via sol–gel technique were observed using a SEM (Fig. 4). The powders had small particle size (~10 nm).Also, Fig. 5 reveals the SEM micrographs of samples A15–A50 with different contents of BTZB addition sintered at 1150 °C and A00 with no BTZB sintered at 1300 °C,which shows us that the grain size of BTZB-doped samples are not uniform, ranging from 0.5 to 1.0 μm. The grain size increases gradually with increasing BTZB content. Compared with conventional sintering aids, nanocomposite sintering aids can be well distributed on the shell of the ceramics with great dispersity and small particle sizes [6, 15].The thickness of the average grain-shell in the ceramics doped with the nano-composite was smaller than in submicron oxide-doped ceramics because of nanocomposite's large specific area, high interfacial energy, and homogeneous distribution on the shell of the ceramics sequentially facilitated the dense matrix sintering of ceramics while keeping the intact ''core–shell'' structure [16, 17].

Figure 5 a shows the microstructure of A15 sample is not compact for there are many pores. With the increasing

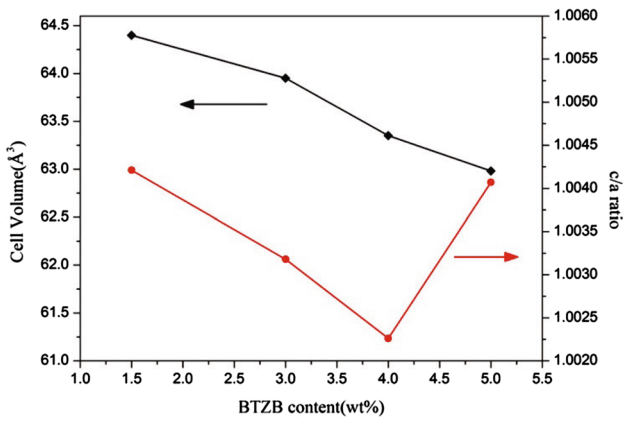

Fig. 3 Unit cell volume and c/a ratio of $BaTiO_3$ ceramics as a function of BTZB content

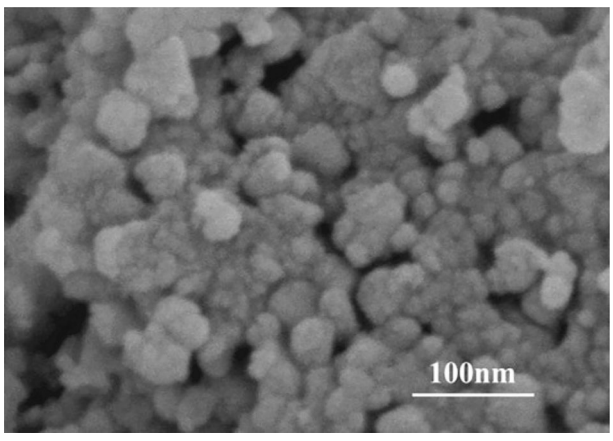

Fig. 4 SEM images of the Bi_2O_3–TiO_2–ZnO–H_2BO_3 powders (calcined at 650 °C)

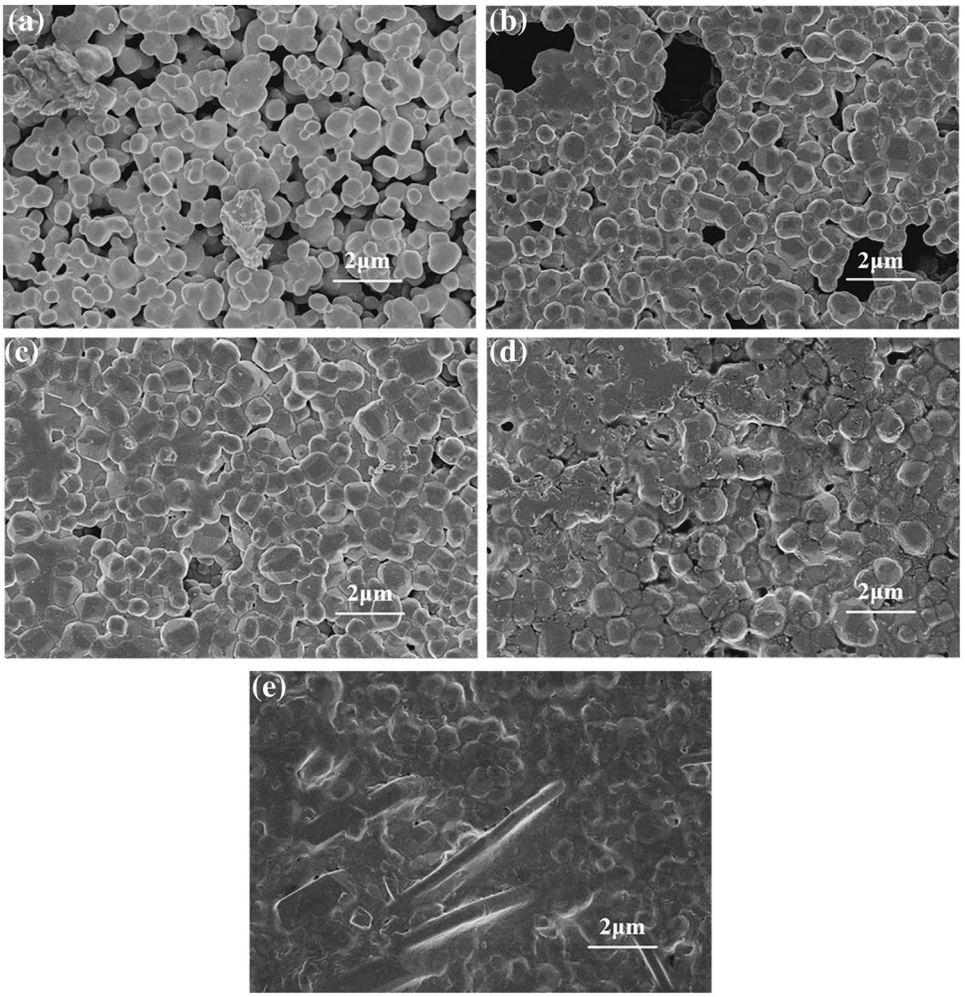

Fig. 5 SEM photos of samples with various amounts of BTZB sintered in 1150 °C: **a** 1.5 wt%; **b** 3.0 wt%; **c** 4.0 wt%; **d** 5.0 wt%, and sample e with no BTZB sintered in 1300 °C

BTZB content (Fig. 5 b, c), the ceramics microstructure become increasingly compact and uniform, and the amounts of pores reduce broadly ,indicated that the doping of BTZB can form a liquid phase during the sintering process as sintering aids, decreasing the distance among grains, and gradually infiltrate into pore channels, which can inhibit the formation of porosity structure [18]. Furthermore, among the samples, A40 is the most predominantly composed of fine grains (<1 μm) with smooth surface and clear boundaries. However, with the continued increasing of BTZB content, excess liquid phase was observed in grain boundaries. This can be interpreted by the grain boundary is known to easily form a eutectic liquid phase [15, 19].

As we can see from Fig. 5 e, sheet grains are observed in the sample A00 without BTZB. However, with the increasing content of BTZB, the sheet grains reduce totally and disappear in the sample A15 ~ A50 with various amounts of BTZB. It can be considered that the sheet grains are second phase mainly consisting of the Ti-rich phase, in keeping with mentioned in the discussion of XRD patterns. Besides, the SEM micrographs results were consistent with the change in XRD patterns. On the other hand, sheet grains are detrimental to the X8R temperature stability, and appropriate BTZB additive content can inhibit the formation of sheet grains effectively [20].

3.3 Dielectric and electrical properties analysis

Main dielectric and electrical properties of samples A00–A50 are listed in Table 1. All samples exhibit low dielectric loss (tan < 1.5%) and sample A15–A50 shows that the room temperature dielectric constant increased with increasing BTZB content. In the case of 4.0 wt% BTZB, the maximum $\varepsilon_{20\,^{\circ}C}$ achieve to 3186. And then in the case of 5.0 wt% BTZB, $\varepsilon_{20\,^{\circ}C}$ began to reduce to 3039.

Besides, the insulation resistivity (ρ_v) in room temperature increase broadly along with the increase of BTZB content, the insulation resistivity of A15 only reach $10^{10}\Omega$ cm as well as A30 A40、A50 rises to $10^{13}\Omega$·cm, especially the sample A50 with 5.0 wt% BTZB, which can be attributed to the improvement of ceramic microstructure for

Table 1 Electrical properties of BTZB-doped $BaTiO_3$ samples in room temperature

Sample	BTZB content (wt%)	ρ(g cm^3)	ρ_v ($10^{13}\Omega$·cm)	$\varepsilon_{20\,°C}$	tanδ (%)	$\Delta C/C_{20}$℃ (%)		
						−55 °C	125 °C	150 °C
A00	0	5.035	18.673	3778	1.114	−13.2	−6.2	−20.6
A15	1.5	4.525	0.00796	1540	1.183	−10	5.3	−3.4
A30	3.0	4.937	1.3899	2754	1.220	−14.6	−2.1	−14.1
A40	4.0	5.359	2.9102	3186	1.384	−12.3	−2.3	−5.6
A50	5.0	5.514	5.0696	3039	1.448	−18.7	6.5	−18.1

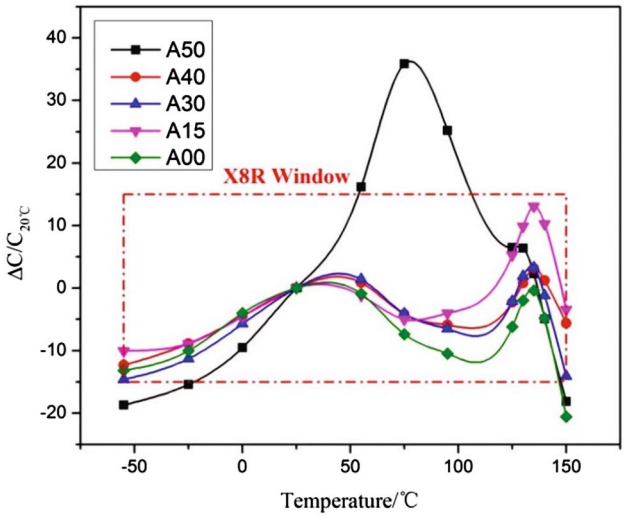

Fig. 6 Temperature dependence of capacitance change for samples A15 ~ A50 with various amounts of BTZB sintered at 1150 °C and A00 with no BTZB sintered at 1300 °C

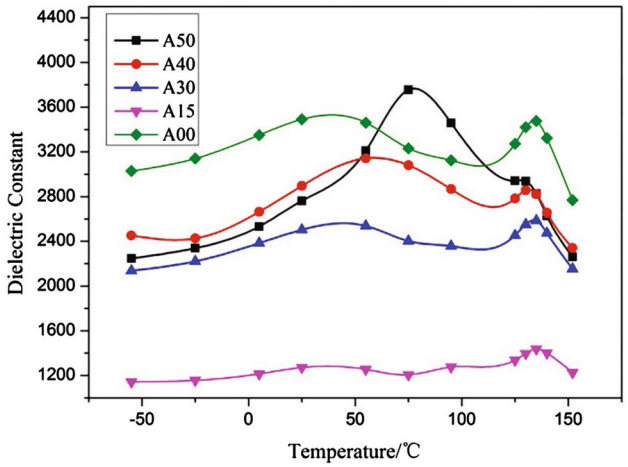

Fig. 7 Temperature dependence of a dielectric constant for samples A15 ~ A50 with various amounts of BTZB sintered at 1150 °C and A00 with no BTZB sintered at 1300°C

$BaTiO_3$ ceramics with a slightly Ti-excess composition were reported to have a higher sintering density. Furthermore, sample A15 showed a low insulation resistivity as $7.96\times10^{10}\Omega$ cm, presumably sample A15 with low content of BTZB wasn't sufficient to make sample densification sintered in 1150 °C.

Figure 6 shows temperature coefficient of capacitance (TCC) curves of samples sintered at 1150 °C for 3 h with the addition of 1.5–5.0 wt% BTZB and A00 with no BTZB sintered at 1300 °C. Which shows an increasing of BTZB content yielded a flat TCC curve, the TCC curves appear two dielectric peaks along with the change of temperature, the peak appears around 45 °C and the dielectric peak appears in 130 °C named Curie peak (Tc).As Fig. 7 shows, dielectric constant is increasing obviously by increasing the content of BTZB, and especially dielectric constant at room temperature ($\varepsilon_{20\,°C}$) which suggesting that when the addition amount of BTZB was small, the liquid that generated during the sintering process was not enough to coat the grain to further accelerate the sintering progress of the ceramics, which causing a reduction of the dielectric property with more pores and low bulk density. With an increasing in the amount of sintering aids, a massive liquid phase was formed and improved densification of ceramic [21, 22].Moreover, sintering aidditive can enhanced particle rearrangement and solution-reprecipitation during liquid-phase sintering, which leading to the mature growth of grains as well as rapid densification of the ceramics, causing an increase in the dielectric constant.

Particularly, Fig. 6 showed that the lower temperature dielectric peak around of 45 °C shifted to high temperature with the increased doping BTZB, when doping content reach 5 wt%,the $\Delta C/C_{20}$-T curve of A50 showed an extraordinary peak around 75 °C, the peak value as high as 37.5%. suggesting that when the concentration of BTZB was excessive, a large liquid phase occurred and accelerated solute transfer, resulting in a rapid change of the microstructure of the ceramics, including abnormal grain growth [23] and grain-shell growth, We deem that BTZB is a nanoscale non-ferroelectric dopant and mainly locates at grain shells, Perhaps a highly mixed phase was deposited at the grain shell layer [24]. The growth of grain-shell caused a high dielectric constant peak around 75 °C. Therefore, to obtain a high dielectric constant with the best compactness,

the optimum doping content of BTZB for X8R-type dielectric ceramics was 4%.

4 Conclusions

A BTZB nano-composite was successfully synthesized via the sol–gel process, X8R ceramics with a high dielectric constant were obtained by sintering with this BTZB nano-composite. The BTZB nanopowders are prepared using the sol–gel method had a nano-scale particle size (~10 nm) and good dispersibility, which was homogeneously dispersed on the shell of $BaTiO_3$-based X8R ceramics. Furthermore, the crystal structure changes gradually from tetragonal to pseudo-cubic with increasing BTZB content, and BTZB can also inhibit the formation of the $Ba_6Ti_{17}O_{40}$ second phase and be favorable to form desired core–shell microstructure in the fine-grained $BaTiO_3$ ceramics.

Moreover, it showed great effects in improving dielectric properties of the $BaTiO_3$-based ceramics by doping BTZB of nanopowders. An increasing of BTZB content yielded a flat TCC curve and obviously increasing of dielectric constant from 1540 to 3169. Sample without BTZB doesn't meet EIA-X8R specification while sample doped with various amounts (1.5wt ~ 4.0 wt%) of BTZB satisfy EIA-X8R temperature characteristic.

In conclusion, the newly developed X8R ceramics doped with 4 wt% BTZB nano-composite reduce the sintering temperature from 1300 to 1150 °C which exhibited a dielectric constant of up to 3186 with a high density, low dielectric loss tan $\delta = 1.384\%$, and flat temperature-capacitance curve $\Delta C/C_{20℃} \leq \pm 15\%$, −55–150 °C, which satisfy EIA-X8R specification.

Acknowledgements This work was supported by the National Natural Science Foundation of China (No. 61671326).

References

1. L.X. Li, J.Y. Yu, N. Zhang, J. Ye, Synthesis and characterization of X8R $BaTiO_3$-based dielectric ceramics by doping with $NiNb_2O_6$ nanopowders. J. Mater. Sci. **26**, 9522–9528 (2015)
2. W.H. Lee, C.Y. Su, Improvement in the temperature stability of a $BaTiO_3$-based multilayer ceramic capacitor by constrained sintering. J. Am. Ceram. Soc. **90**, 3345–3348 (2007)
3. Y.B. Chen, B. Yuan, The dielectric properties of $0.85MgTiO_3$–$0.15Ca_{0.6}La_{0.8/3}TiO_3$ with ZnO additions for microwave applications. J. Alloys Compd. **477**, 883–887 (2009)
4. S.F. Wang, Y.R. Wang, Y.C. Wu, Y.J. Liu, Densification, microstructural evolution, and dielectric properties of hexagonal $Ba(Ti_{1-x}Mn_x)O_3$ ceramics sintered with fluxes. J. Alloys Compd. **480**, 499–504 (2009)
5. S.H. Choi, Y.N. Ko, J.H. Kim, Y.J. Hong, Y.C. Kang, Characteristics of BaO–B_2O_3–SiO_2 nano glass powders prepared by flame spray pyrolysis as the sintering agent of $BaTiO_3$ ceramics. J. Alloys Compd. **509**, 7979–7984 (2011)
6. R. Niu, B. Cui, F. Du, Z. Chang, Z. Tang, Synthesis and characterization of Zn–B–Si–O nano-composites and their doped $BaTiO_3$ ceramics. Mater. Res. Bull. **45**, 1460–1465 (2010)
7. P. Gao, H. Ji, Q. Jia, X. Li, Low temperature sintering and dielectric properties of $Ba_{0.6}Sr_{0.4}TiO_3$–MgO composite ceramics with CaO–B_2O_3–SiO_2 glass addition. J. Alloys Compd. **527**, 90–95 (2012)
8. T.A. Jain, C.C. Chen, K.Z. Fung, Effects of $Bi_4Ti_3O_{12}$ addition on the microstructure and dielectric properties of Mn-doped BaTiO3-based X8R ceramics. J. Alloys Compd. **476**, 414–419 (2009)
9. H.I. Hsiang, C.S. Hsi, C.C. Huang, S.L. Fu, Sintering behavior and dielectric properties of $BaTiO_3$ ceramics with glass addition for internal capacitor of LTCC. J. Alloys Compd. **459**, 307–310 (2008)
10. J.B. Lim, S. Zhang, N. Kim, High-temperature dielectrics in the $BiScO_3$–$BaTiO_3$–$(K_{1/2}Bi_{1/2})TiO_3$ ternary system. J. Am. Ceram. Soc. **92**, 679–682 (2009)
11. C.L. Freeman, J.A. Dawson, H.R. Chen, T.R. Shrout, A new potential model for barium titanate and its implications for rare-earth doping. J. Mater. Chem. **21**. 4861–4868 (2011)
12. X. Xu, G.E. Hilmas, Effects of $Ba_6Ti_{17}O_{40}$ on the dielectric properties of Nb-doped $BaTiO_3$ ceramics. J. Am. Ceram. Soc. **89**, 2496–2501 (2006)
13. L. Li, Y. Liu, B. Cui, R. Niu, Q. Zhang, Z. Chang, Enhancement of dielectric properties by addition of Li–Ti–Si–O nanocomposite to X7R ceramics. J. Alloys Compd. **550**, 216–220 (2013)
14. T.A. Jain, C.C. Chen, K.Z. Fung, Effects of $Bi_4Ti_3O_{12}$ addition on the microstructure and dielectric properties of modified $BaTiO_3$ under a reducing atmosphere. J. Eur. Ceram. Soc. **29**, 2595–2601 (2009)
15. P.P. Phule, S.H. Risbud, Low-temperature synthesis and processing of electronic materials in the BaO–TiO_2 system. J. Mater. Sci. **25**, 1169–1183 (1990)
16. Y. Yuan, S. Zhang, W. You, Preparation of $BaTiO_3$-based X7R ceramics with high dielectric constant by nanometer oxides doping method. Mater. Lett. **58**, 1959–1963 (2004)
17. X. Zhou, S. Zhang, Y. Yuan, B. Li, J. Liu, Preparation of $BaTiO_3$-based nonreducible X7R dielectric materials via nanometer powders doping. J. Mater. Sci. **17**, 133–136 (2006)
18. J.C.C. Lin, W.C.J. Wei, Low-temperature sintering of $BaTiO_3$ with Mn-Si-O glass. J. Electroceram. **25**, 179–187 (2010)
19. K.J. Park, C.H. Kim, Y.J. Yoon, S.M. Song, Y.T. Kim, Doping behaviors of dysprosium, yttrium and holmium in $BaTiO_3$ ceramics. J. Eur. Ceram. Soc. **29**, 1735–1741 (2009)
20. L. Li, M. Wang, Y. Liu, J. Chen, N. Zhang, Decisive role of MgO addition in the ultra-broad temperature stability of multi-component $BaTiO_3$-based ceramics. Ceram. Int. **40**, 1105–1110 (2014)
21. S.F. Wang, T.C.K. Yang, Y.R. Wang, Y. Kuromitsu, Effect of glass composition on the densification and dielectric properties of $BaTiO_3$ ceramics. Ceram. Int. **27**, 157–162 (2001)
22. H.I. Hsiang, T.H. Chen, Influence of glass additives on the sintering behavior and dielectric properties of $BaO{\cdot}(Nd_{0.8}Bi_{0.2})_2O_3{\cdot}4TiO_2$ ceramics. J. Alloys Compd. **467**, 485–490 (2009)
23. Y.C. Lee, W.H. Lu, S.H. Wang, C.W. Lin, Effect of SiO_2, addition on the dielectric properties and microstructure of $BaTiO_3$-based ceramics in reducing sintering. Int. J. Miner. Metall. Mater. **16**, 124–127 (2009)
24. J.C.C. Lin, W.C.J. Wei, Melting and interface reaction of Mn–Si–O glass on $BaTiO_3$. J. Am. Ceram. Soc. **92**, 1926–1933 (2009)